

## Review Article

Open Access, Volume 2

# In vivo imaging tools for functional assessment of biomaterials implanted bone regeneration

Subhasis Roy<sup>1</sup>; Prasenjit Mukherjee<sup>1</sup>; Samit Kumar Nandi<sup>2\*</sup>

<sup>1</sup>Assistant Professor, Department of Veterinary Clinical Complex, F/O. VAS, WBUAFSc, Kolkata 37, India.

<sup>2</sup>Professor, Department of Veterinary Surgery and Radiology, F/O. VAS, WBUAFSc, Kolkata 37, India.

### \*Corresponding Author: Samit Kumar Nandi

Professor, Department of Veterinary Surgery and Radiology, West Bengal University of Animal and Fishery Sciences, 37 & 68 K. B. Sarani, Kolkata 37, India.

Email: samitnandi1967@gmail.com

Received: Oct 16, 2021

Accepted: Dec 16, 2021

Published: Dec 23, 2021

Archived: www.jcimcr.org

Copyright: © Nandi SK (2021).

DOI: www.doi.org/10.52768/2766-7820/1504

### Abstract

Since the discovery of X-rays and its first use in imaging of a hand, bone tissue has been the chapter of interest in medical imaging. However, X-ray imaging poses limitations nowadays owing to the augmented complexity of implant scaffolds as well as with the advances in bone engineering. As a result, advanced follow-up imaging techniques are of paramount necessity for effective postoperative characterization. Moreover, it is also needed to search for non-invasive, high-sensitivity, and high-resolution structural, functional, and molecular imaging techniques such as acoustic, optical, magnetic, X-Ray, electron, ultrasound, and nuclear imaging, etc. as an alternative to normally used X-ray computed tomography. Further, enthusiastic preclinical scanners have turned out to be accessible, with sensitivity and resolution even superior to clinical scanners, as a consequence helping a rapid transformation from preclinical to clinical applications. Besides, recently, bone-specific probes and contrast agents are developing for better imaging tools in bone-tissue engineering applications. This review highlights such emerging preclinical imaging tools, each with its individual potencies and flaws, either used only or in combination. In particular, multimodal imaging will significantly add to improve the present understanding in the characterization of bone regenerative processes.

**Keywords:** bone tissue engineering; biomaterials imaging; modern technologies; acoustic; magnetic; nuclear imaging.

### Introduction

Bone, the highly vascularized connective tissue, is mainly composed of hydroxyapatite, calcium carbonate, and phosphate which account for two-thirds of the total bone. The rest of the part is composed of collagen, proteoglycans, and other non-collagen proteins including different growth factors and morphogenic proteins with a significant amount of water [1]. These altogether provide the mechanical strength of the bone as well as provide its flexibility. Most of the bones are composed of the outer cortical bone and the inner spongy bone. Bone heals without forming any scar tissues. The process of bone healing may be delayed due to different pathological conditions lead-

ing to nonunion, malunion, and other bone infections. Hence, disabled healing conditions sometimes necessitate the application of bone graft. A bone graft may be defined as a material that is implanted for promoting the healing process. The graft material may be used alone or in combination with other materials. The main objective of healing is to bring osteogenesis, osteoinduction, and osteoconduction. Nowadays nanotechnology has been extensively studied in the field of orthopedic and is being used successfully for challenging bone surgery or infections. Nano scaffolds, delivery methods, controlled alteration of surface geography and composition, and bio microelectro mechanical systems are examples of some nanotechnology of applications in orthopedic surgery [2].

**Citation:** Roy S, Mukherjee P, Nandi SK. In vivo imaging tools for functional assessment of biomaterials implanted bone regeneration. *J Clin Images Med Case Rep.* 2021; 2(6): 1504.

The use of nano-technology in biologic research is studied vividly for its unique nature of exceptionally small size, surface functionality and well-matching with cellular components. This technology also helps to upgrade the mechanical strength of scaffold biomaterials to optimize the bone healing responses. Surface modification of the implants has been proved to improve the healing response also [3].

With the advancement of tissue engineering technology, different strategies for nanomaterial construction have also been evolved [4-6]. Hence, these technological applications need to be assessed by varied imaging approaches which will not only be evaluating its morphological aspect but also its functional and molecular information. Amongst numerous technologies, one conventional method like histological techniques lacks detailed information, more preciously in vivo studies [4] and destruction of the samples. To overcome such limitations of conventional technologies, different advanced imaging modalities with the features of noninvasive, longitudinal, and constant supervising of the implant/constructs have emerged and now are used successfully [5-7].

Ideal imaging methods must 1. Determine signals at the sub-cellular level and enter the whole body and 2. Provide contrast to explore all the vital data including morphological, physiological, and molecular changes [8]. There are, at present, no such ideal techniques that have all these qualities. Hence, the use of different technology is needed and requirement-based. Actually, the imaging tools are functioning based on the interaction of construct/cellular part and imaging energy sources and detect the energy change and emitted by the cells for the formation of an image. Spatial and temporal resolution, diffusion depth, relevant endogenous and exogenous contrast agents, protection, and price are the different parameters that are closely related to modern tissue imaging tools' specifications [9-12]. Different technologies along with their characteristics and other modalities have been presented in Table 1.

X-ray and Computed Tomography (CT), Positron Emission Tomography (PET) and Single-Photon Emission Computed Tomography (SPECT), Magnetic Resonance Imaging (MRI), Ultrasound Imaging (US), Optical Imaging (OI) are few examples of different modern imaging technologies for assessing tissues/organs/implants, etc. The tissue and implant imaging techniques help the researchers to evaluate the host-graft interaction along with immune reaction against implants and scaffolds. These also help to indicate and follow the signal release cascades [13]. All the available techniques may be divided into two categories; one will provide information on anatomical aspects (CT, MRI, US) and the other will highlight metabolic aspects (PET, SPECT, OI). These modern biomedical imaging techniques greatly increased spatial resolution, infiltration depth, temporal response, recognition understanding, and element specificity along with providing biomaterials-cell contrast and characterization at the interface site [1]. In this review advantages and disadvantages of different technologies along with better visualization of interactions in physical background aimed with need-based, perspective will be discussed. This manuscript will be immensely helpful to the biomaterial and biomedical researchers to choose their required technology for the characterization of tissue-implant interactions, immune reaction to the grafts, implants and scaffolds.

### Functional assessment of osteogenic biomaterials

Unlike most other tissues, the bone itself can regenerate and repair itself without forming any scar. There are certain situations where this process may be hampered. Inadequate blood supply, osteomyelitis and soft tissue infections, systemic diseases affecting healing, instability of fracture ends are some of such conditions which may lead to mal or nonunion. Different phases and events of normal bone healing have been presented in Table 2.

**Table 1:** Different modern imaging technologies with their attributes.

Imaging methods	Micro-PET	Micro-CT	Micro-MRI	Micro ultrasound	OCT	Optical microscopy	Bioluminescence	Photoacoustics
<b>Properties</b>								
<b>Imaging depth</b>	Full body	Full body	Full body	10 mm	1-3 mm	0.3–1.0 mm	10 mm	20 mm
<b>Spatial resolution</b>	1–2 mm	5 µm	5-200 µm	20-100 µm	1-15 µm	0.2-1 µm	2-3 mm	50-150 µm
<b>Real-time</b>	No	No	Yes	Yes	Yes	Yes	Yes	Yes
<b>Anatomy</b>	Poor	Excellent	Excellent	Very good	Good	Poor	Poor	good
<b>Endogenous contrast: blood</b>	Poor	Poor	Very good	Good	Poor	Very good	Poor	Excellent
<b>Endogenous contrast: bone</b>	Good	Excellent	Very good	Poor	Good	Very good	Poor	Poor
<b>Blood perfusion</b>	Poor	Poor	Excellent	Good	Poor	Poor	Poor	Excellent
<b>Oxygen saturation</b>	Poor	Poor	Very good	Poor	Poor	Poor	Poor	Excellent
<b>Molecular imaging using contrast agent</b>	Excellent	Poor	Very good	Good	Good	Excellent	Excellent	Excellent
<b>Cost</b>	High	Medium	High	Low	Low	Low	Low	Medium
<b>Portability</b>	Low	Low	Low	High	High	High	High	High
<b>Contrast mechanism</b>	Gamma ray emission	X-ray absorption	Proton magnetization and relaxation	Acoustic reflection (back scattering)	Optical back scattering	Light		Optical absorption
<b>Advantages</b>	Noninvasive, deep penetration, high molecular sensitivity	Noninvasive, deep penetration, high resolution	Noninvasive, deep penetration	Noninvasive, high speed, deep penetration	Noninvasive, cellular-level resolution, high imaging speed	Can observe living cells, and a wide range of biological activity, not affected by electromagnetic field	Noninvasive, <i>in vivo</i> studies of infection, cancer progression	Noninvasive, high practical and element sensitivity, deep infiltration

<b>Limitations</b>	Low resolution, radiative labeling	Ionizing radiation, low chemical sensitivity	Expensive, low imaging speed	small resolution and chemical sensitivity, coupling medium required	Superficial penetration, low chemical sensitivity	lacks resolution	May not offer an accurate depiction of the biological outcome, inadequate and wavelength-dependent diffusion of light through animal tissues.	Coupling medium needed
<b>Application areas</b>	Cell metabolism, cell tracking	Engineered bone, pore structures	Fluid content and transport	Mechanics, flow dynamics, scaffold cavitation	Vascularization, cell tracking, scaffold degradation	Biological/cellular events. Gross cellular changes.	Detection of lung inflammation, pulmonary metastasis	Vascularization, oxygenation, cell tracking, cell-biomaterial interaction

Adopted from references [4,9-12,14,15]

**Table 2:** Healing events of bone tissue.

	0-5 day	5-10 day	10-16 day	16-21 day	21-35 day
<b>Events</b>	Hematoma [16,17]	Soft callus	Fibrous tissue [18]	Hard callus [16]	Remodeled bone [17]
<b>Major cell predominates</b>	Macrophage, B-cell [19] Stem cells	Chondrocyte, osteoblast [20]	Hypertrophic Chondrocyte [21], osteoclast [22], Macrophage [23]	Myelopoietic and hematopoietic cells [24]	Osteocyte [1]

Different biomaterials and implantable grafts are popularly being used to treat bone healing abnormalities. A perfect bone graft should possess osteoinducing, osteoconducting, and osteointegrating properties for efficient incorporation into the host bone tissue [13]. Osteoconduction is osteoblast stimulation by Bone Morphogenetic Proteins (BMP), growth factors and MSCs. Osteoconduction is to provide scaffold bed for new bone growth into. Osseointegration is host bone-implant bonding [25-27]. Assessment of healing is one of the indicative parameters to propose or to expect normal repair of the bone defect. Metabolomics assays like TNF-470 [28], expression of mRNA by in situ hybridization [29], individual mRNA assay [30-33], Micro Array approaches [34-39], evaluation of osteoblastic proliferation including type I collagen, osteocalcin, osteonectin, osteopontin, bone sialoprotein [40], alkaline phosphatase level [45], identification of monoclonal antibodies like SB10 [40] and HOP 26 [41], marking of cells of the osteogenic lineage using retroviral-mediated gene transfer [42], molecular probe-based implant evaluation for modulation of osteogenic process [40,41,43,44] are examples of some common assessment methods which are frequently used to evaluate biomaterials' osteointegration and bone healing.

There are some *in vivo* experimental models like segmental/calvarial bone defect, subcutaneous placement of demineralized bone matrix/material [45-50] and diffusion chamber model [51,52] which are also used to evaluate osteointegration properties of the implanted biomaterials.

Apart from histology, histomorphometry is also used as a valuable tool for the evaluation of bone tissue construct.

### Histology

This technique is being used since long back and is successfully been employed to evaluate the attributes and changes of bone cells and scaffolds. Generally, light microscopy is helpful for this reason but the use of a digital pathology slide scanner is the best option for a rapid and high-resolution image. The use of this modified scanner will convert the glass slide into a digital slide and one can see the image at a different real optical image [53]. With the help of this technique tissue morphology, fibrosis, necrosis, inflammatory changes, neo-vascularization, fatty changes, mineralization, new bone formation, bone density, quality, and materials degradation can be measured. His-

tology of both decalcified and undecalcified implanted bone sections can be performed to assess the bone regeneration at the implantation side as well as to study the activities of biodegradable materials (Figure 1a) [54-56]. In decalcified bone specimens, the microtome cut paraffin embedded and hematoxylin and eosin stained sections are observed in light microscope fitted with a digital camera and connected to a computer for assessing the cellular response with the host bone to the implants [57]. Similarly in undecalcified bone samples, dehydrated, Spurr's resin embedded perpendicular bone sections stained with Masson Goldner's trichrome are observed under light microscope connected with digital camera and computer to evaluate the behaviour of implanted biomaterials.

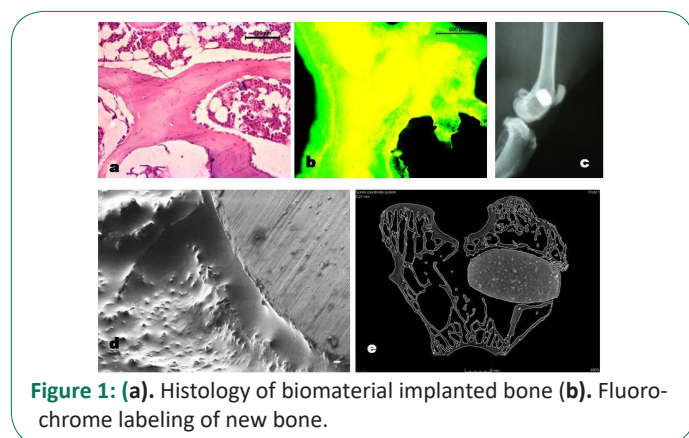


**Figure 1:** (a). Histology of biomaterial implanted bone (b). Fluorochrome labeling of new bone.

**Histomorphometry:** Histomorphometric examination from bone samples is generally carried out to measure the extent of newly formed osseous tissue, presence of remaining graft particles, and non-mineralized tissue. This robust analysis technique provides quantitative numerical data on bone microarchitecture, remodeling, and metabolism [58]. Histomorphometry also provides an insight into bone properties of certain skeletal conditions like osteomalacia, osteoporosis, etc. although this method provides accurate data, the expense, and requirement of time are the main hindrances. To overcome such problems, a semi-automated quantification method was adopted to measure trabecular area, osteoid area, trabecular thickness, and osteoclast activity using ImageJ toolbox and plugins (Bone J) software [59]. Details of the sample preparation, image capturing, and evaluation was nicely mentioned (Figure 2)[59].

Unlike bone histology, this technique also provides exact disease characterization and response to treatment and information on bone remodeling in a quantitative manner rather than qualitative [60]. It can be useful to the histological figures or to the high-resolution images obtained by different modern techniques. Baddeley *et al.* [61] and Vesterby *et al.* [62] worked on histomorphometry based on stereological formula assuming random and unbiased sampling. Now different techniques of measurement like Bioquant and Osteometrics ([www.bioquant.com](http://www.bioquant.com), [www.osteometrics.com](http://www.osteometrics.com).) are available with modern facilities of measurement. Different researchers also used this method for evaluating bone tissue and constructs [63,64]. Pathophysiology of metabolic bone diseases is also well studied by this technology [65-67].

All the modern imaging modalities work on the principles of energy interactions of imaging source with the implanted biomaterials and tissues [14] which mostly includes absorption, scattering and polarization. Depending on the contrast medium, the imaging technologies may be grouped as acoustic, optical, magnetic, X-Ray, electron, and nuclear imaging.

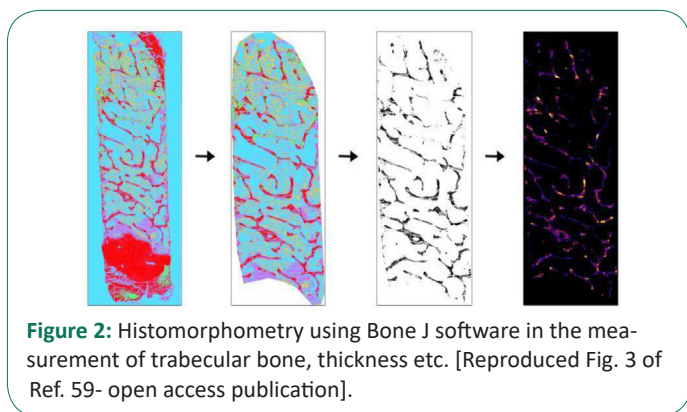


**Figure 2:** Histomorphometry using Bone J software in the measurement of trabecular bone, thickness etc. [Reproduced Fig. 3 of Ref. 59- open access publication].

### Acoustic imaging techniques

#### Ultrasonography

Three Dimensional anatomical configurations may be obtained from ultrasonographical interventions of the tissues [68,69]. Ultrasonography is the safest imaging method owing to the fact of its lower wave length and higher penetration and may be employed for scaffold material characterization [70] as well as to screen material degradation, and calculate the role and organization of vasculature. The imaging of biomaterials and tissues depends on different attributes of ultrasonography like mass density, modulus, and cavitation. Depending on the above factors, the following modes of application is usually employed to study the intended part; B Mode for mineralization [71], Doppler imaging for vascular study [72], ultrasonic elastography for scaffold degradation [69], microbubble mediated sonography for the study of drug delivery or gene therapy [73], plain ultrasonography, etc.. This technique lacks of radiation and is of low cost with the facility of portability.

#### Optical

Optical Imaging (OI) is the oldest technique with high sensitivity that can create 2D images by passing visible light through thin objects. This modality lacks better depth visualization. This procedure works on the principle of photon detection. Most of biomedical laboratories prefer to use this modality owing to its flexible imaging contrasts and high spatial resolutions. Following are the different types of OI techniques

**Fluorescence imaging (FLI):** Fluorescent microscopy meth-

ods allow assessing cellular relations, tissue function, and in some cases helps to examine tissue engineered biomaterials in situ with the use of fluorophores and without the necessity of exogenous labels. Different fluorescent dye for imaging bone regeneration is commercially available like high-affinity bisphosphonate-based bone agents and tetracycline derivatives targeting bone [1]. One of the fluorescent marker is tetracycline that follows the ionized calcium and are deposited the site of active bone mineralization during the healing process. New bone formation at the implanted site can be seen with bright golden yellow fluorescence in the green background (Figure 1b). This can be assessed using a Fluorescence microscope connected with digital camera, computer and source of U-V light. The new bone formation can be quantified by measuring the golden yellow pixels inbuilt with the computer system. During the imaging process, the sections should be placed close to the surface and/or set in a particular optically translucent window chamber. Hydrogel-based scaffolds are predominantly a difficult subject for imaging owing to their elevated water content. However, alteration of hydrogels with a fluorescent tag allows screening of degradation of in vitro and subcutaneously implanted *in vivo* bioimplants [74].

**Fluorescence molecular tomography (FMT):** Cathepsin K targeting probe is used to target osteoclastic activity [75]. Using this technology, it is likely to quantify each discrete source detector-pairs at the cost of an extended measurement time. [76,77]

**Bioluminescence imaging (BLI):** Bone repair is measured by the use of luciferase-bearing transgenic Mice [70,78]. Through this technology, it is easier to evaluate transgene expression, progress of infection, tumor progress and metastasis, transplantation, toxicology, viral infections, and gene therapy [79]. De'gano *et al.*, used this technique to assess the *in vivo* bone regeneration ability of implanted human bone marrow and adipose tissue MSCs, loaded arginine-glycine-aspartate crosslinked hydrogel scaffold in mouse calvarial defects over a period of 12-week. He observed that luciferase-labeled cells could be monitored *in vivo* for a prolonged period. [78]

**Confocal microscopy (CM):** It is mainly used for imaging of tissue and scaffold materials [80]. Using this technology in the second near-infrared (NIR-II) window, it has been established that bone is a vital organ for the retention of nanoparticles. Small polymer nanoparticles of ~15 nm diameter displayed fast buildup and long-standing retention in bone. This technique helps to identify the dispersion of nanoparticles in the endothelial cells of sinusoidal vessels in bone marrow [81]. In modern machines technology like NIR-II *in vivo* imaging system equipped with an 808-nm laser and an InGaAs camera (Photonic Science, UK) is available where emission is collected with 1319 nm long-pass filter.

**Multiphoton microscopy (MPM):** This technique can be used for biomaterial and tissue visualization [80], and cells of bone marrow [82]. Multiphoton microscopy can be employed even without adding fluorescent molecules to enable cells to be imaged like many other approaches. For imaging of biological samples, a femtosecond laser must be used. Multiphoton microscopy is a commanding tool for high-resolution imaging in a 3D sample that is optically opaque. It also helps to visualize the *in vivo* vibrant movement of osteoclasts and osteoblasts, in addition to their interactions with each other [83]. To understand the mechanism of interactions between implanted biomaterials and vascular micro atmosphere in a cranial bone defect window

chamber mice model, multiphoton laser scanning microscopy is a useful technique that offers high-resolution, four-dimensional imaging analyses [84]. The same imaging tool was successfully used to assess the osseous tissue regeneration on BMSC-mediated calvarial bone defect repair [85,86]. Another advantage of this technique is that it permits to take chronological *in vivo* images of bone tissue-engineered constructs with high temporal and spatial resolution for more extensive periods without disturbing the biological phenomena [87].

**Photoacoustic tomography (PAT):** Measures *in vivo* oxygenation saturation of hemoglobin along with evaluation of tissue angiogenesis [5,88]. Tissues are irradiated by pulsed laser light which ultimately leads to production of pressure waves caused by temperature and volume. Generally, NIR and visible light is used in PAT [89].

**Intravital microscopy:** Intravital microscopy is a visualization of individual cells in living condition [90]. It mandatorily needs implantation of imaging window in the animal under study [91]. The key benefit of this technique is that it can visualize the cells in living mode and the cellular activities can be recorded in real mode. If the image resolution is high, it is practically possible to make 3D images of individual cells through this technique. Specific fluorescent labeling is necessary to record the cellular events by this process. The main disadvantage of this technique is that it cannot visualize all cell types as the distinguished fluorescence levels are not available for all the cell types. Osteocytic osteolysis progressions in bone have been documented by Eleonora *et al.* [92] and Hiroshige *et al.* [93] by using this technology. Hemodynamics and Vascular Permeability of mouse bone marrow were studied by Yookyung *et al.* [94] with this modality. The role of microvasculature for bone healing in normal and perturbed bone was documented by Winet [95] with the help of this technique (Figure 3).

To track peri-implant endosseous healing, Intravital imaging plays a vital role to calculate angiogenesis and perivascular cell dynamics that happens around orthopedic and dental implants. This new imaging technique has been used to assess bone angiogenesis and cellular dynamics during bone defect repair [86,96,97]. However, scanty information on high-resolution *in vivo* longitudinal reports is available to study peri-implant angiogenesis. Of late, Khosravi *et al.*, 2018 developed a novel technique to quantify the vascular and cellular changes around the bone implants using an intravital imaging approach [98]. This technique can also be employed to as imaging tools for ectopic bone formation in bone-tissue regeneration [84].

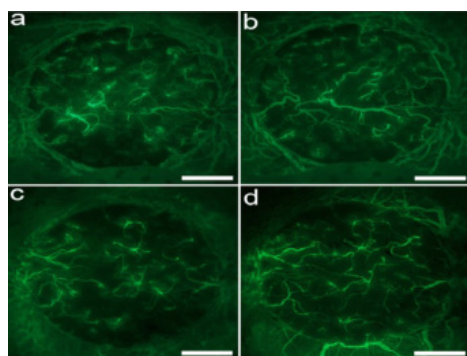


**Figure 3:** Intravital microscopy of Fluorescence images shows vessel generation at the BCP implanted cranial window defect area using intravenous injection of FITC dextran. (a, c-at 14 days; b, d-at 28 days) [Reproduce eCM journal with acknowledgement-Open access paper Ref. 53]

**Optical coherence tomography (OCT):** It measures the structural changes of the scaffold in the 3D mode which might be due to degradation of scaffold or matrix deposition [99]. It is based on low-coherence interferometry, characteristically using near-infrared light.

### X-Ray, electron, and nuclear imaging of material structures at several scales

#### Conventional X-ray

Among the diverse non-invasive characterization parameters, the conventional X-ray study is one of the best methods to assess the bone-implant interaction as well as mechanical interlocking (Figure 1c) [55]. This technique also provides valuable insight into the degradation kinetics of implanted scaffold within the bone defect [54]. The gradual reduction of radio-opacity states degradation of implants vis-à-vis new bone tissue regeneration [100]. Although X-ray-based imaging provides excellent resolution, and is very fast, however, needs ionizing radiation and thus can potentially damage implanted implants. Phase contrast x-ray shows better sensitivity to image polymer scaffolds [101].

#### Electron microscopy (EM)

It consists of Scanning Electron microscopy (SEM) and Transmission Electron microscopy (TEM). It is the best modality that can provide the highest resolution image of cell-scaffold interface. These images can provide details like scaffold pore size, fiber orientation, cell deposition, and interface interactions. It actually used for nanoscale characterization of biomaterials. This technology is costly and very limited capacity to provide images of the specimens containing live cells (Figure 1d) [102].

**Nuclear imaging:** It is one type of ionizing imaging modality that detects photons emitted from either isotope or from radiotracers [103]. This process does not produce any toxicity. It can penetrate deep tissues even a whole-body scan is also possible. It can detect radio-labeled cells or tissues or substances at the nano or pico-molar level. Nuclear imaging has poor spatial resolution capacity owing to the scattering of gamma rays by tissues; hence MRI or CT is advised in association with gaining better architectural and molecular information. It includes Positron Emission Tomography (PET) and Single-Photon Emission Computed Tomography (SPECT).

**SPECT:** In this system commonly  $^{99m}\text{Tc}$ ,  $^{111}\text{In}$ ,  $^{125}\text{I}$  gamma ( $\gamma$ ) emitting radioisotopes are used [104]. This modality uses multiple energy windows at the same time, hence different radioisotopes labeled tracers may be injected simultaneously. Diphosphonates labeled with  $^{99m}\text{Tc}$  radioisotopes have a longer half-life than any other used in nuclear imaging, thus more easily to trace the healing process of bone by much fewer periodic injections of radiotracers.

**PET CT:** It is generally employed to monitor the cell metabolism using a radioactive glucose analog ( $^{18}\text{F}$ -fluorodeoxyglucose). In this scanning modality, two oppositely directed annihilation photons by positron ( $\beta^+$ ) emitting isotopes are identified over time concurrence by a pair of detectors. Dynamic PET Compartmental analysis enables to absolutely quantify the tracer bone uptake and can evaluate the comparative osteoblastic activity [105,106]. The cost of PET instrumentation is much more due to the establishment of a cyclotron unit for production of radioisotopes. CT scan generally offered standard anatomic information whereas PET illustrated the higher new bone formation at the

implanted defect site. Since bone regeneration encompasses a vibrant interaction of biological processes, dynamic PET-CT imaging is thought to be an appropriate means for real-time tracking of the amount and rate of bone formation.

In nuclear imaging, the most common disadvantage is that the radioisotopes which are generally used have a very short half-life hence repeated injections; once per week, are generally necessary to trace or track the events of bone healing. Another drawback is its inability to differentiate the osteoblastic activity between scaffolds induced with host tissue made [8,106]. To summarize, PET imaging provides higher contrast of the osteoblastic activity at the defect area as compared to SPECT, which might be due to the better spatial resolution of PET scanners.

### Micro CT

Micro-CT (mCT) has been utilized to illustrate the internal organization of a broad range of engineering scaffolds before use at *in vivo* situations. This technique is the most accepted method of characterization of tissue engineered scaffold implanted bone owing to its highly absorbing properties of mineralized tissues. It can measure the details of internal structure of bone at both macro and micro levels. Here subjects are scanned in different angles and ultimately converted to a 3D image (Figure 1e). Bone density, surface area details, vasculature, osteocytic identification all can be measured by this noninvasive method in conjunction with contrast agent and synchrotron-radiation micro-CT. Factors like movement artifacts and cumulative radiation are to be considered while using this technique [70,107,108].

**Magnetic imaging:** Magnetic Resonance Imaging (MRI) is employed for the characterization of fluid [109] and hence very challenging to image the bone as its water content is less. MRI is usually employed to monitor cartilage [110], adipose tissue [111], vascularization [112] and exo or endogenous contrast [113]. Application of MRI for tracking of stem cell differentiation and degradation [114–116] and *in vivo* biomaterials interactions study in small animals [117] is also evident in the literature. In MRI different imaging sequences are used like T1 and T2 weighted. It varies depending on the part under investigation. In MRI, T1 weighted sequences are commonly employed for adipose tissue, blood moving at slow speed, paramagnetic contrast media which are formed by short echo (TE) and repetition (TR) times. In contrast, T2 uses longer TE and TR. As the bone contains no free protons, bone appears black as gives no signal. Thus modifications of this modality to semi-quantitative MRI approaches have been evoked for evaluating hard tissues which are as follows a. Nuclear Magnetic Resonance (NMR) spectroscopy b. Ultra-Short Echo Time (UTE) c. Zero Echo Time (ZTE) d. Sweep Imaging With Fourier Transformation (SWIFT) [70,107,108].

### Conclusion

Current biomedical imaging modalities have reformed the research with images of detailed architectural, operational and molecular information of tissue constructs having a high spatial resolution, deep infiltration, greater temporal sensitivity, and better elemental specificity. More and more developments in the field of instrumentation and techniques are ongoing for characterizing bone scaffold materials along with the host tissue reactions against the construct. Previously, unattained tissues or biomaterials can be visualized with different technologies. Of late, much more modifications again strengthen the

responsiveness of tissue under study by application of CLARITY and Expansion Microscopy (ExM). In CLARITY tissue clearing techniques are employed for better clear resolution whereas in ExM tissues are physically expanded 4-5 times for attaining higher resolution. In spite of remarkable progress in imaging technologies, several considerations for further developments have to be taken into considerations like super-resolution techniques in the US, improved depth in OI, technologies for accelerated imaging with high resolutions in X-ray, and nuclear imaging modalities. The growth and developments in the sector of biomedical engineering will ultimately help the researchers to select the appropriate tissue construct with more detailed knowledge and skill.

### Declarations

**Acknowledgement:** The authors acknowledge reproducing one figure (Figure 3 in this manuscript) from the [www.ecmjournal.org](http://www.ecmjournal.org) and article figure no 3 of Wernike et al 2010, 19 <http://wap.ecmjournal.org/journal/papers/vol019/pdf/v019a04.pdf>. The authors also acknowledge the kind support of the Vice-Chancellor, West Bengal University of Animal and Fishery Sciences, Kolkata, India.

**Conflict of interests:** The authors declare that there is no conflict of interest in this manuscript.

### References

1. Fragogeorgi EA, Rouchota M, Georgiou M, Velez M, Bouziotis P, et al. *In vivo* imaging techniques for bone tissue engineering. *J Tissue Eng.* 2019; 10: 2041731419854586.
2. Harvey EJ, Henderson JE, Vengallatore ST. Nanotechnology and Bone Healing. *J Orthop Trauma.* 2010; 24: S25.
3. Staples M, Daniel K, Cima MJ, Langer R. Application of Micro- and Nano-Electromechanical Devices to Drug Delivery. *Pharm Res.* 2006; 23: 847–63.
4. Appel AA, Anastasio MA, Larson JC, Brey EM. Imaging challenges in biomaterials and tissue engineering. *Biomaterials* 2013; 34: 6615–6630.
5. Cai X, Zhang YS, Xia Y, Wang LV. Photoacoustic microscopy in tissue engineering. *Mater Today.* 2013; 16: 67–77.
6. Appel A, Anastasio MA, Brey EM. Potential for Imaging Engineered Tissues with X-Ray Phase Contrast. *Tissue Eng Part B Rev.* 2011; 17: 321–30.
7. Guagliardi A, Giannini C, Cedola A, Mastrogiacomo M, Ladisa M, Cancedda R. Toward the X-Ray Microdiffraction Imaging of Bone and Tissue-Engineered Bone. *Tissue Eng Part B Rev.* 2009; 15: 423–442.
8. Nam SY, Ricles LM, Suggs LJ, Emelianov SY. Imaging strategies for tissue engineering applications. *Tissue Eng Part B Rev.* 2015; 21: 88–102.
9. Pysz MA, Gambhir SS, Willmann JK. Molecular imaging: Current status and emerging strategies. *Clin Radiol* 2010; 65: 500–516.
10. Georgakoudi I, Rice WL, Hronik Tupaj M, Kaplan DL. Optical Spectroscopy and Imaging for the Noninvasive Evaluation of Engineered Tissues. *Tissue Eng Part B Rev.* 2008; 14: 321–340.
11. Rahmim A, Zaidi H. PET versus SPECT: Strengths, limitations and challenges. *Nucl Med Commun.* 2008; 29: 193–207.
12. Massoud TF, Gambhir SS. Molecular imaging in living subjects: seeing fundamental biological processes in a new light. *Genes Dev.* 2003; 17: 545–580.

13. Oryan A, Alidadi S, Moshiri A, Maffulli N. Bone regenerative medicine: Classic options, novel strategies, and future directions. *J Orthop Surg.* 2014; 9: 18.
14. Zhang YS, Yao J. Imaging Biomaterial–Tissue Interactions. *Trends Biotechnol.* 2018; 36: 403–414.
15. Sadikot RT, Blackwell TS. Bioluminescence imaging. *Proc Am Thorac Soc.* 2005; 2: 537–40, 511–2.
16. Mountziaris PM, Mikos AG. Modulation of the Inflammatory Response for Enhanced Bone Tissue Regeneration. *Tissue Eng Part B Rev.* 2008; 14: 179–186.
17. Thomson DD. Introduction–Mechanisms of fracture healing and pharmacologic control. *J Musculoskelet Neuronal Interact.* 2003; 3: 295–296.
18. Oryan A, Monazzah S, Bigham-Sadegh A. Bone injury and fracture healing biology. *Biomed Environ Sci BES.* 2015; 28: 57–71.
19. LaStayo PC, Winters KM, Hardy M. Fracture healing: Bone healing, fracture management and current concepts related to the hand. *J Hand Ther.* 2003; 16: 81–93.
20. Goldhahn J, Féron JM, Kanis J, Papapoulos S, Reginster JY, Rizzoli R, et al. Implications for Fracture Healing of Current and New Osteoporosis Treatments: An ESCEO Consensus Paper. *Calcif Tissue Int.* 2012; 90: 343–353.
21. Geris L, Gerisch A, Sloten JV, Weiner R, Oosterwyck HV. Angiogenesis in bone fracture healing: A bioregulatory model. *J Theor Biol.* 2008; 251: 137–158.
22. Haverstock BD, Mandracchia VJ. Cigarette smoking and bone healing: Implications in foot and ankle surgery. *J Foot Ankle Surg.* 1998; 37: 69–74.
23. Schindeler A, McDonald MM, Bokko P, Little DG. Bone remodeling during fracture repair: The cellular picture. *Semin Cell Dev Biol.* 2008; 19: 459–466.
24. Lauzon MA, Bergeron É, Marcos B, Fauchoux N. Bone repair: New developments in growth factor delivery systems and their mathematical modeling. *J Controlled Release.* 2012; 162: 502–520.
25. Zimmermann G, Moghaddam A. Allograft bone matrix versus synthetic bone graft substitutes. *Injury.* 2011; 42: S16–21.
26. Kneser U, Schaefer DJ, Polykandriotis E, Horch RE. Tissue engineering of bone: The reconstructive surgeon's point of view. *J Cell Mol Med.* 2006; 10: 7–19.
27. Nandi SK, Roy S, Mukherjee P, Kundu B, De DK, Basu D. Orthopaedic applications of bone graft & graft substitutes: A review. *Indian J Med Reseach.* 2010; 132: 15–30.
28. Hausman MR, Schaffler MB, Majeska RJ. Prevention of fracture healing in rats by an inhibitor of angiogenesis. *Bone.* 2001; 29: 560–564.
29. Gerstenfeld LC, Alkhiary YM, Krall EA, Nicholls FH, Stapleton SN, Fitch JL, et al. Three-dimensional Reconstruction of Fracture Callus Morphogenesis. *J Histochem Cytochem.* 2006; 54: 1215–1228.
30. Kon T, Cho T-J, Aizawa T, Yamazaki M, Nooh N, Graves D, et al. Expression of Osteoprotegerin, Receptor Activator of NF- $\kappa$ B Ligand (Osteoprotegerin Ligand) and Related Proinflammatory Cytokines During Fracture Healing. *J Bone Miner Res.* 2001; 16: 1004–1014.
31. Jepsen KJ, Price C, Silkman LJ, Nicholls FH, Nasser P, Hu B, et al. Genetic Variation in the Patterns of Skeletal Progenitor Cell Differentiation and Progression During Endochondral Bone Formation Affects the Rate of Fracture Healing. *J Bone Miner Res.* 2008; 23: 1204–1216.
32. Kakar S, Einhorn TA, Vora S, Miara LJ, Hon G, Wigner NA, et al. Enhanced Chondrogenesis and Wnt Signaling in PTH Treated Fractures. *J Bone Miner Res.* 2007; 22: 1903–1912.
33. Palomares KTS, Gerstenfeld LC, Wigner NA, Lenburg ME, Einhorn TA, Morgan EF. Transcriptional profiling and biochemical analysis of mechanically induced cartilaginous tissues in a rat model. *Arthritis Rheum.* 2010; 62: 1108–1118.
34. Hadjiargyrou M, Lombardo F, Zhao S, Ahrens W, Joo J, Ahn H, et al. Transcriptional Profiling of Bone Regeneration: INSIGHT INTO THE MOLECULAR COMPLEXITY OF WOUND REPAIR \* 210. *J Biol Chem.* 2002; 277: 30177–30182.
35. Wang K, Vishwanath P, Eichler GS, Al-Sebaei MO, Edgar CM, Einhorn TA, et al. Analysis of fracture healing by large-scale transcriptional profile identified temporal relationships between metalloproteinase and ADAMTS mRNA expression. *Matrix Biol.* 2006; 25: 271–281.
36. Rundle CH, Wang H, Yu H, Chadwick RB, Davis EI, Wergedal JE, et al. Microarray analysis of gene expression during the inflammation and endochondral bone formation stages of rat femur fracture repair. *Bone.* 2006; 38: 521–529.
37. Bais M, McLean J, Sebastiani P, Young M, Wigner N, Smith T, et al. Transcriptional Analysis of Fracture Healing and the Induction of Embryonic Stem Cell–Related Genes. *PLOS ONE.* 2009; 4: e5393.
38. Wise JK, Sena K, Vranizan K, Pollock JF, Healy KE, Hughes WF, et al. Temporal Gene Expression Profiling during Rat Femoral Marrow Ablation-Induced Intramembranous Bone Regeneration. *PLOS ONE.* 2010; 5: e12987.
39. Grimes R, Jepsen KJ, Fitch JL, Einhorn TA, Gerstenfeld LC. The transcriptome of fracture healing defines mechanisms of coordination of skeletal and vascular development during endochondral bone formation. *J Bone Miner Res.* 2011; 26: 2597–2609.
40. Bilezikian JP, Raisz LG, Martin TJ. Principles of Bone Biology. Academic Press; 2008.
41. Bruder SP, Horowitz MC, Mosca JD, Haynesworth SE. Monoclonal antibodies reactive with human osteogenic cell surface antigens. *Bone.* 1997; 21: 225–235.
42. Oreffo ROC, Triffitt JT. In vitro and in vivo methods to determine the interactions of osteogenic cells with biomaterials. *J Mater Sci Mater Med.* 1999; 10: 607–611.
43. Stein GS, Lian JB. Molecular mechanisms mediating proliferation/differentiation interrelationships during progressive development of the osteoblast phenotype. *Endocr Rev.* 1993; 14: 424–442.
44. Neo M, Voigt CF, Herbst H, Gross UM. Analysis of osteoblast activity at biomaterial-bone interfaces by in situ hybridization. *J Biomed Mater Res.* 1996; 30: 485–492.
45. Horisaka Y, Okamoto Y, Matsumoto N, Yoshimura Y, Kawada J, Yamashita K, et al. Subperiosteal implantation of bone morphogenetic protein adsorbed to hydroxyapatite. *Clin Orthop* 1991: 303–312.
46. Johnson EE, Urist MR, Finerman GA. Resistant nonunions and partial or complete segmental defects of long bones. Treatment with implants of a composite of human bone morphogenetic protein (BMP) and autolyzed, antigen-extracted, allogeneic (AAA) bone. *Clin Orthop.* 1992: 229–237.
47. Yasko AW, Lane JM, Fellingner EJ, Rosen V, Wozney JM, Wang EA.

- The healing of segmental bone defects, induced by recombinant human bone morphogenetic protein (rhBMP-2). A radiographic, histological, and biomechanical study in rats. *J Bone Joint Surg Am.* 1992; 74: 659–670.
48. Ohgushi H, Goldberg VM, Caplan AI. Heterotopic osteogenesis in porous ceramics induced by marrow cells. *J Orthop Res.* 1989; 7: 568–578.
  49. Ripamonti U. Osteoinduction in porous hydroxyapatite implanted in heterotopic sites of different animal models. *Biomaterials.* 1996; 17: 31–35.
  50. Ripamonti U, Ma SS, Reddi AH. Induction of bone in composites of osteogenin and porous hydroxyapatite in baboons. *Plast Reconstr Surg.* 1992; 89: 731–739.
  51. Bruder SP, Gazit D, Passi-Even L, Bab I, Caplan AI. Osteochondral differentiation and the emergence of stage-specific osteogenic cell-surface molecules by bone marrow cells in diffusion chambers. *Bone Miner.* 1990; 11: 141–151.
  52. Takaoka T, Okumura M, Ohgushi H, Inoue K, Takakura Y, Tamai S, et al. Histological and biochemical evaluation of osteogenic response in porous hydroxyapatite coated alumina ceramics. *Biomaterials.* 1996; 17: 1499–1505.
  53. Maglio M, Salamanna F, Brogini S, Borsari V, Pagani S, Nicoli Aldini N, et al. Histological, Histomorphometrical, and Biomechanical Studies of Bone-Implanted Medical Devices: Hard Resin Embedding. *Bio Med Res Int.* 2020; 2020: e1804630.
  54. Devi KB, Tripathy B, Kumta PN, Nandi SK, Roy M. In Vivo Biocompatibility of Zinc-Doped Magnesium Silicate Bio-Ceramics. *ACS Biomater Sci Eng.* 2018; 4: 2126–2133.
  55. Nandi SK, Fielding G, Banerjee D, Bandyopadhyay A, Bose S. 3D-printed  $\beta$ -TCP bone tissue engineering scaffolds: Effects of chemistry on in vivo biological properties in a rabbit tibia model. *J Mater Res.* 2018; 33: 1939–1947.
  56. Dasgupta S, Maji K, Nandi SK. Investigating the mechanical, physicochemical and osteogenic properties in gelatin-chitosan-bioactive nanoceramic composite scaffolds for bone tissue regeneration: In vitro and in vivo. *Mater Sci Eng C.* 2019; 94: 713–728.
  57. Moses JC, Nandi SK, Mandal BB. Multifunctional Cell Instructive Silk-Bioactive Glass Composite Reinforced Scaffolds Toward Osteoinductive, Proangiogenic, and Resorbable Bone Grafts. *Adv Healthc Mater.* 2018; 7: 1701418.
  58. Fernandes GVO, Calasans-Maia M, Mitri FF, Bernardo VG, Rossi AM, Almeida GDS, et al. Histomorphometric Analysis of Bone Repair in Critical Size Defect in Rats Calvaria Treated with Hydroxyapatite and Zinc-Containing Hydroxyapatite 5%. *Key Eng Mater.* 2009; 396–398: 15–8.
  59. Malhan D, Muelke M, Rosch S, Schaefer AB, Merboth F, Weisweiler D, et al. An Optimized Approach to Perform Bone Histomorphometry. *Front Endocrinol.* 2018; 0.
  60. Compston J, Skingle L, Dempster DW. Chapter 53 - Bone Histomorphometry. In: Feldman D, editor. *Vitam.* Fourth Ed., Academic Press; 2018, 959–973.
  61. Baddeley AJ, Gundersen HJG, Cruz-Orive LM. Estimation of surface area from vertical sections. *J Microsc.* 1986; 142: 259–276.
  62. Vesterby A, Kragstrup J, Gundersen HJG, Melsen F. Unbiased stereologic estimation of surface density in bone using vertical sections. *Bone.* 1987; 8: 13–17.
  63. Maréchal M, Luyten F, Nijs J, Postnov A, Schepers E, Steenbergh D van. Histomorphometry and micro-computed tomography of bone augmentation under a titanium membrane. *Clin Oral Implants Res.* 2005; 16: 708–714.
  64. Chappard D, Retailleau-Gaborit N, Legrand E, Baslé MF, Audran M. Comparison Insight Bone Measurements by Histomorphometry and  $\mu$ CT. *J Bone Miner Res* 2005; 20: 1177–1184.
  65. Reid IR, Miller PD, Brown JP, Kendler DL, Fahrleitner-Pammer A, Valter I, et al. Effects of denosumab on bone histomorphometry: The FREEDOM and STAND studies. *J Bone Miner Res* 2010; 25: 2256–2265.
  66. Recker RR, Delmas PD, Halse J, Reid IR, Boonen S, García-Hernandez PA, et al. Effects of Intravenous Zoledronic Acid Once Yearly on Bone Remodeling and Bone Structure. *J Bone Miner Res.* 2008; 23: 6–16.
  67. Recker RR, Ste-Marie L-G, Langdahl B, Czerwinski E, Bonvoisin B, Masanaukaite D, et al. Effects of intermittent intravenous ibandronate injections on bone quality and micro-architecture in women with postmenopausal osteoporosis: The DIVA study. *Bone* 2010; 46: 660–665.
  68. Talukdar Y, Avti P, Sun J, Sitharaman B. Multimodal Ultrasound-Photoacoustic Imaging of Tissue Engineering Scaffolds and Blood Oxygen Saturation In and Around the Scaffolds. *Tissue Eng Part C Methods.* 2014; 20: 440–449.
  69. Yu J, Takanari K, Hong Y, Lee K-W, Amoroso NJ, Wang Y, et al. Non-invasive characterization of polyurethane-based tissue constructs in a rat abdominal repair model using high frequency ultrasound elasticity imaging. *Biomaterials.* 2013; 34: 2701–2709.
  70. Ventura M, Boerman OC, de Korte C, Rijpkema M, Heerschap A, Oosterwijk E, et al. Preclinical Imaging in Bone Tissue Engineering. *Tissue Eng Part B Rev.* 2014; 20: 578–595.
  71. Gudur M, Rao RR, Hsiao Y-S, Peterson AW, Deng CX, Stegemann JP. Noninvasive, Quantitative, Spatiotemporal Characterization of Mineralization in Three-Dimensional Collagen Hydrogels Using High-Resolution Spectral Ultrasound Imaging. *Tissue Eng Part C Methods.* 2012; 18: 935–946.
  72. Kang K-T, Allen P, Bischoff J. Bioengineered human vascular networks transplanted into secondary mice reconnect with the host vasculature and re-establish perfusion. *Blood.* 2011; 118: 6718–6721.
  73. Bez M, Sheyn D, Tawackoli W, Avalos P, Shapiro G, Giaconi JC, et al. In situ bone tissue engineering via ultrasound-mediated gene delivery to endogenous progenitor cells in mini-pigs. *Sci Transl Med.* 2017; 9.
  74. Artzi N, Oliva N, Puron C, Shitreet S, Artzi S, bon Ramos A, et al. In vivo and in vitro tracking of erosion in biodegradable materials using non-invasive fluorescence imaging. *Nat Mater.* 2011; 10: 890–890.
  75. Lambers FM, Kuhn G, Müller R. Advances in multimodality molecular imaging of bone structure and function. *Bone Key Rep.* 2012; 1: 37.
  76. Ntziachristos V, Tung C-H, Bremer C, Weissleder R. Fluorescence molecular tomography resolves protease activity in vivo. *Nat Med.* 2002; 8: 757–761.
  77. Ntziachristos V, Weissleder R. Charge-coupled-device based scanner for tomography of fluorescent near infrared probes in turbid media. *Med Phys.* 2002; 29: 803–809.
  78. Décano IR, Vilalta M, Bagó JR, Matthies AM, Hubbell JA, Dimitriou H, et al. Bioluminescence imaging of calvarial bone repair using bone marrow and adipose tissue-derived mesenchymal stem cells. *Biomaterials.* 2008; 29: 427–437.



79. Wetterwald A, van der Pluijm G, Que I, Sijmons B, Buijs J, Karperien M, et al. Optical Imaging of Cancer Metastasis to Bone Marrow: A Mouse Model of Minimal Residual Disease. *Am J Pathol.* 2002; 160: 1143–1153.
80. Kolewe ME, Park H, Gray C, Ye X, Langer R, Freed LE. 3D Structural Patterns in Scalable, Elastomeric Scaffolds Guide Engineered Tissue Architecture. *Adv Mater.* 2013; 25: 4459–4465.
81. Chen D, Liu Y, Zhang Z, Liu Z, Fang X, He S, et al. NIR-II Fluorescence Imaging Reveals Bone Marrow Retention of Small Polymer Nanoparticles. *Nano Lett.* 2021; 21: 798–805.
82. Hawkins ED, Duarte D, Akinduro O, Khorshed RA, Passaro D, Nowicka M, et al. T-cell acute leukaemia exhibits dynamic interactions with bone marrow microenvironments. *Nature.* 2016; 538: 518–522.
83. Hashimoto K, Kaito T, Kikuta J, Ishii M. Intravital imaging of orthotopic and ectopic bone. *Inflamm Regen.* 2020; 40: 26.
84. Zhang X. Intravital Imaging to Understand Spatiotemporal Regulation of Osteogenesis and Angiogenesis in Cranial Defect Repair and Regeneration. In: Singh SR, Rameshwar P, editors. *Somat. Stem Cells Methods Protoc.*, New York, NY: Springer; 2018; 229–239.
85. Villa MM, Wang L, Huang J, Rowe DW, Wei M. Visualizing Osteogenesis In Vivo Within a Cell–Scaffold Construct for Bone Tissue Engineering Using Two-Photon Microscopy. *Tissue Eng Part C Methods.* 2013; 19: 839–849.
86. Huang C, Ness VP, Yang X, Chen H, Luo J, Brown EB, et al. Spatiotemporal Analyses of Osteogenesis and Angiogenesis via Intravital Imaging in Cranial Bone Defect Repair. *J Bone Miner Res.* 2015; 30: 1217–1230.
87. Stiers P-J, Gastel N van, Moermans K, Stockmans I, Carmeliet G. An Ectopic Imaging Window for Intravital Imaging of Engineered Bone Tissue. *JBMR Plus.* 2018; 2: 92–102.
88. Pan D, Pramanik M, Senpan A, Allen JS, Zhang H, Wickline SA, et al. Molecular photoacoustic imaging of angiogenesis with integrin-targeted gold nanobeacons. *FASEB J.* 2011; 25: 875–82.
89. Schelkanova I, Pandya A, Muhaseen A, Saiko G, Douplik A. 13 - Early optical diagnosis of pressure ulcers. In: Meglinski I, editor. *Biophotonics Med. Appl.*, Woodhead Publishing; 2015; 347–75.
90. Masedunskas A, Milberg O, Porat-Shliom N, Sramkova M, Wigand T, Amornphimoltham P, et al. Intravital microscopy. *Bio-Architecture.* 2012; 2: 143–157.
91. Ritsma L, Steller EJA, Beerling E, Loomans CJM, Zomer A, Gerlach C, et al. Intravital Microscopy Through an Abdominal Imaging Window Reveals a Pre-Micrometastasis Stage During Liver Metastasis. *Sci Transl Med.* 2012; 4: 158ra145–158ra145.
92. Dondossola E, Alexander S, Holzapfel BM, Filippini S, Starbuck MW, Hoffman RM, et al. Intravital microscopy of osteolytic progression and therapy response of cancer lesions in the bone. *Sci Transl Med.* 2018; 10.
93. Sano H, Kikuta J, Furuya M, Kondo N, Endo N, Ishii M. Intravital bone imaging by two-photon excitation microscopy to identify osteocytic osteolysis in vivo. *Bone.* 2015; 74: 134–9.
94. Jung Y, Spencer JA, Raphael AP, Wu JW, Alt C, Runnels JR, et al. Intravital Imaging of Mous Bone Marrow: Hemodynamics and Vascular Permeability. *Methods Mol Biol Clifton NJ.* 2018; 1763: 11–22.
95. Winet H. The role of microvasculature in normal and perturbed bone healing as revealed by intravital microscopy. *Bone* 1996; 19: S39–57.
96. Park D, Spencer JA, Lin CP, Scadden DT. Sequential In vivo Imaging of Osteogenic Stem/Progenitor Cells During Fracture Repair. *JoVE J Vis Exp.* 2014: e51289.
97. Tavassol F, Kampmann A, Schumann P, Lindhorst D, Kokemüller H, Essig H, et al. A Novel Approach for Studying Microcirculation in Bone Defects by Intravital Fluorescence Microscopy. *Tissue Eng Part C Methods.* 2011; 17: 1151–1159.
98. Khosravi N, Mendes VC, Nirmal G, Majeed S, DaCosta RS, Davies JE. Intravital Imaging for Tracking of Angiogenesis and Cellular Events Around Surgical Bone Implants. *Tissue Eng Part C Methods.* 2018; 24: 617–627.
99. Liang X, Graf BW, Boppart SA. Imaging engineered tissues using structural and functional optical coherence tomography. *J Biophotonics.* 2009; 2: 643–655.
100. Samanta SK, Devi KB, Das P, Mukherjee P, Chanda A, Roy M, et al. Metallic ion doped tri-calcium phosphate ceramics: Effect of dynamic loading on in vivo bone regeneration. *J Mech Behav Biomed Mater.* 2019; 96: 227–235.
101. Zhu N, Chapman D, Cooper D, Schreyer DJ, Chen X. X-Ray, et al. Diffraction Enhanced Imaging as a Novel Method to Visualize Low-Density Scaffolds in Soft Tissue Engineering. *Tissue Eng Part C Methods.* 2011; 17: 1071–1080.
102. Kim U-J, Park J, Joo Kim H, Wada M, Kaplan DL. Three-dimensional aqueous-derived biomaterial scaffolds from silk fibroin. *Biomaterials* 2005; 26: 2775–2785.
103. Kofidis T, Lenz A, Boublik J, Akhyari P, Wachsmann B, Mueller-Stahl K, et al. Pulsatile perfusion and cardiomyocyte viability in a solid three-dimensional matrix. *Biomaterials.* 2003; 24: 5009–5014.
104. Skaliczki G, Weszl M, Schandl K, Major T, Kovács M, Skaliczki J, et al. Compromised bone healing following spacer removal in a rat femoral defect model. *Acta Physiol Hung.* 2012; 99: 223–232.
105. Cheng C, Alt V, Dimitrakopoulou-Strauss A, Pan L, Thormann U, Schnettler R, et al. Evaluation of New Bone Formation in Normal and Osteoporotic Rats with a 3-mm Femur Defect: Functional Assessment with Dynamic PET-CT (dPET-CT) Using 2-Deoxy-2-[18F]Fluoro-D-Glucose (18F-FDG) and 18F-Fluoride. *Mol Imaging Biol* 2013; 15: 336–344.
106. Wong KK, Piert M. Dynamic Bone Imaging with 99mTc-Labeled. Diphosphonates and 18F-NaF: Mechanisms and Applications. *J Nucl Med.* 2013; 54: 590–599.
107. Tremoleda JL, Khalil M, Gompels LL, Wylezinska-Arridge M, Vincent T, Gsell W. Imaging technologies for preclinical models of bone and joint disorders. *EJNMMI Res.* 2011; 1: 11.
108. Trachtenberg JE, Vo TN, Mikos AG. Pre-clinical Characterization of Tissue Engineering Constructs for Bone and Cartilage Regeneration. *Ann Biomed Eng.* 2015; 43: 681–696.
109. Xu H, Othman SF, Magin RL. Monitoring Tissue Engineering Using Magnetic Resonance Imaging. *J Biosci Bioeng.* 2008; 106: 515–527.
110. Kotecha M, Klatt D, Magin RL. Monitoring Cartilage Tissue Engineering Using Magnetic Resonance Spectroscopy, Imaging, and Elastography. *Tissue Eng Part B Rev.* 2013; 19: 470–484.
111. Xu J, Chen Y, Yue Y, Sun J, Cui L. Reconstruction of epidural fat with engineered adipose tissue from adipose derived stem cells and PLGA in the rabbit dorsal laminectomy model. *Biomaterials.* 2012; 33: 6965–6973.
112. Beaumont M, DuVal MG, Loai Y, Farhat WA, Sándor GK, Cheng H-LM. Monitoring angiogenesis in soft-tissue engineered con-

---

structs for calvarium bone regeneration: an in vivo longitudinal DCE-MRI study. *NMR Biomed.* 2010; 23: 48–55.

113. Bible E, Dell'Acqua F, Solanky B, Balducci A, Crapo PM, Badylak SF, et al. Non-invasive imaging of transplanted human neural stem cells and ECM scaffold remodeling in the stroke-damaged rat brain by 19F- and diffusion-MRI. *Biomaterials.* 2012; 33: 2858–2871.
114. Roeder E, Henrionnet C, Goebel JC, Gambier N, Beuf O, Grenier D, et al. Dose-Response of Superparamagnetic Iron Oxide Labeling on Mesenchymal Stem Cells Chondrogenic Differentiation: A Multi-Scale In Vitro Study. *PLOS ONE.* 2014; 9: e98451.
115. Mertens ME, Frese J, Bölükbas DA, Hrdlicka L, Golombek S, Koch S, et al. FMN-Coated Fluorescent USPIO for Cell Labeling and Non-Invasive MR Imaging in Tissue Engineering. *Theranostics.* 2014; 4: 1002–1013.
116. Leferink AM, van Blitterswijk CA, Moroni L. Methods of Monitoring Cell Fate and Tissue Growth in Three Dimensional Scaffold Based Strategies for In Vitro Tissue Engineering. *Tissue Eng Part B Rev.* 2016; 22: 265–283.
117. Hsueh Y-S, Chen Y-S, Tai H-C, Mestak O, Chao S-C, Chen Y-Y, et al. Laminin-Alginate Beads as Preadipocyte Carriers to Enhance Adipogenesis In Vitro and In Vivo. *Tissue Eng Part A.* 2017; 23: 185–194.